Estimating dark matter halo concentration from the integrated mass profile

C. Poveda $\star$[1] J. E. Forero-Romero †[1] J. C. Muñoz-Cuartas ‡[2]

[1]*Departamento de Física, Universidad de los Andes, Cra. 1 No. 18A-10, Edificio Ip, Bogotá, Colombia*
[2]*Instituto de Física - FCEN, Universidad de Antioquia, Calle 67 No. 53-108, Medellín, Colombia*

1 November 2015

ABSTRACT

Here we show that the concentration parameter in dark matter halos from N-body simulations can be reliably estimated from the radially integrated mass profile. The main advantage of this method is that it uses the full particle information without any binning, **which makes it very switable in cases when resolution becomes important**. We test our method both on mock and N-body halos to compare it against two popular methods to find concentrations: maximum radial velocity measurements and radial particle binning to **fit the density profile**. Tests on the mock halos show that the accuracy of our method to recover input concentrations varies with the halo **resolution**. For halos sampled with 20 particles our method recovers the input concentration with 10% accuracy. **For the maximum radial velocity method it is on the order of** 20% **while density profile methods perform worst at the low resolution limit since they require at least 200 particles inside the virial radius to make a reliable estimate of the density profile**. For halos with 2×10^4 particles our method achieves an accuracy of 0.01% while the velocity and density profile methods achieve 0.1% and 1%, respectively. We measure the mass-concentration relationship on N-body data taking care of using halos sampled with at least 200 particles. We find that at low masses $10^{12}h^{-1}\mathrm{M}_\odot < M < 10^{13}h^{-1}\mathrm{M}_\odot$ our method yields median concentration values lower by a $15\% - 20\%$ compared to the velocity and density methods (**why?**). At higher masses $3\times10^{13}h^{-1}\mathrm{M}_\odot < M < 2\times10^{14}h^{-1}\mathrm{M}_\odot$ the three methods give similar results.

Key words: Cosmology: theory - large-scale structure of Universe - Methods: data analysis - numerical - N-body simulations

1 INTRODUCTION

In the concordance cosmological paradigm the matter content of the Universe is dominated by dark matter, a collisionless fluid shaped by gravitational interactions. In the last three decades simulations of dark matter dominated universes have provided valuable insights into the large scale structure formation process, showing a remarkable success in the comparison between theoretical results and observations of the galaxy distribution obtained from surveys. (Springel et al. 2005; Klypin et al. 2011).

Navarro et.al. 2010 have used high resolution simulations to show that the full halo density profile is not universal and follows an Einasto density distribution. However, if one is not interested in the very central region of the dark matter halo (where galaxy formation takes place, and where the effects of baryon physics on dark matter distribution is still an uncknown), one can assume an approximation where dark matter overdensities closely follow an universal density profile. In a first approximation this profile is spherically symmetric and its density only dependens on the radial coordinate. Although it is well known that the characteristics of this density profile depends on redshift (Maccio et.al. 2008), its universal shape seems to be independent of the cosmological parameters and is self-similar for different spatial scales after an adequate re-scaling is applied. (Navarro et al. 1997; Taylor & Navarro 2001)

In such circumstances, one the most popular parameterizations for dark matter halo radial density distribution is the Navarro-Frenk-White (NFW) profile (Navarro et al.

$\star$ cn.poveda542@uniandes.edu.co
† je.forero@uniandes.edu.co
‡ xxxx@udea.edu.co

1997). This profile is a double power law in radius, where the transition break happens at the so-called scale radius, r_s. The ratio between the scale radius and the virial radius R_v is known as the concentration $c = R_v/r_s$. Simulations show that the concentration is a strong function of halo mass and redshift and provides information about the mass assembly of the dark matter halo (Citar paper que reproduce mis graficas y conecta C con m(z)).

Observationally, the relationship between halo mass and concentration could provide a potential test of the Cold Dark Matter (CDM) paradigm on galactic scales. For this motivation a great deal of effort has been invested in calibrating this relationship with simulations (Neto et al. 2007; Duffy et al. 2008; Muñoz-Cuartas et al. 2011; Prada et al. 2012; Ludlow et al. 2014) and finding the best possible way to constraint it with observations (Buote et al. 2007; Comerford & Natarajan 2007; Mandelbaum et al. 2008; Giocoli et al. 2014; Foëx et al. 2014; Shan et al. 2015).

In N-body simulations there are two main methods to estimate the concentration parameter of a dark matter halo in a N-body simulation. The first method takes the particles composing the halos and bins them in logarithmic radii to estimate the density in each bin, then it proceeds to fit the density as a function of the radius to the NFW profile. A second method uses an analytic property of the NFW profile that relates the maximum of the ratio of the circular velocity to the virial velocity. The concentration can be then found as the root of a algebraic equation dependent on this maximum value.

The first method is straightforward to apply but presents two disadvantages. First, it requires a large number of particles in order to have a proper density estimate in each bin. This makes the method robust only for halos with at least 10^3 particles. The second problem is that there is not a way to estimate the optimal radial bin size, different choices produce different results for the concentration.

The second method solves the two problems mentioned above. It works with low particle numbers and does not involve data binning. However, it effectively takes into account only a single data point and discards the behaviour of the ratio $V_{\rm circ}/V_{\rm vir}$ below and above its maxima. Additionally, small fluctuations on the value of this maximum can yield large perturbations on the estimated concentration parameter.

In this paper we propose a new method to estimate the dark matter halo concentration in halos from N-body simulations. Our method builds the cumulative mass profile from the particle to find the best possible concentration value fitting this distribution. This proposal has two advantages with respect to the two methods mentioned above. It does not involve any data binning and does not throw away data points **resulting in a robust estimate even at low resolution/particle numbers. In the same sence, since the method does not require any binning, there is no need to tune numerical parameters, which provide definitive/independent estimates for the concentration parameter.**.

mi opinin es que el mtodo es muy bueno, y sobresalta sobre los otros dos en sus ventaja: robusto, no requiere bineo, aplica bien en resoluciones pobres. Como herramienta (que es lo que se est vendiendo en el trabajo, un mtodo, eso es lo que hay que recalcar y resaltar)

2   BASIC PROPERTIES OF THE NFW DENSITY PROFILE

Let us review first the basic properties of the NFW density profile. This shall help us to define our notation and review the important assumptions of the two different methods commonly used to measure the concentration to finally present the new method.

2.1   Density profile

The NFW density profile can be written as

$$\rho(r) = \frac{\rho_c \delta_c}{r/r_s(1 + r/r_s)^2}, \tag{1}$$

where $\rho_c \equiv 3H^2/8\pi G$ is the Universe critical density, H is the Hubble constant, G and the universal gravitational constant, δ_c is the halo dimensionless characteristic density and r_s is the scale radius. This radius marks **the point where the logarithmic slope of the density profile is equal to -2** marking the transition between the power law scaling $\rho \propto r^{-1}$ for $r < r_s$ and $\rho \propto r^{-3}$ for $r > r_s$.

We define the virial radius of a halo, r_v, as the boundary of the spherical volume that encloses a density of Δ_h times the mean density of the Universe. The corresponding mass M_v, the virial mass, can be written as $M_v = \frac{4\pi}{3}\bar{\rho}\Delta_h r_v^3$. From these virial quantities we define new dimensionless variables for the radius and mass $x \equiv r/r_v$ and $m \equiv M(< r)/M_v$.

In this paper we use $\Delta_h = 740$ roughly corresponding to 200 times the critical density **at redshift z=0**.

2.2   Integrated mass profile

From these definitions we can compute the total mass enclosed inside a radius r:

$$M(< r) = 4\pi\rho_c \delta_c r_s^3 \left[\ln\left(\frac{r_s + r}{r_s}\right) - \frac{r}{r_s + r}\right], \tag{2}$$

or in terms of the dimensionless mass and radius variables

$$m(< x) = \frac{1}{A}\left[\ln\left(1 + xc\right) - \left(\frac{xc}{xc + 1}\right)\right], \tag{3}$$

where

$$A = \ln\left(1 + c\right) - \left(\frac{c}{c + 1}\right), \tag{4}$$

and the parameter c corresponds to the concentration $c \equiv r_v/r_s$.

From this normalization value and for later convenience we define the following function

$$f(x) = \ln\left(1 + x\right) - \left(\frac{x}{x + 1}\right). \tag{5}$$

The most interesting feature of Eq. (3) is that the concentration is the only free parameter to describe the integrated mass profile.

2.3 Circular velocity profile

It is also customary to express the mass of the halo in terms of the circular velocity $V_c = \sqrt{GM(<r)/r}$. From this we can define a new dimensionless circular velocity $v(<x) \equiv V_c(<r)/V_c(<r_v)$, using the result in Eq. 3 to have:

$$v(<x) = \sqrt{\frac{1}{A} \left[\frac{\ln(1+xc)}{x} - \frac{c}{xc+1} \right]}, \qquad (6)$$

This normalized profile always shows a maximum provided that the concentration is larger than $c > 2$. It is possible to show that for the NFW profile the maximum is provided by

$$\max(v(<x)) = \sqrt{\frac{c}{x_{max}} \frac{f(x_{max})}{f(c)}}, \qquad (7)$$

where $x_{max} = 2.163$ (Klypin et al. 2014) and the function $f(x)$ was defined in Eq. (5).

3 METHODS TO ESTIMATE THE CONCENTRATION FROM N-BODY SIMULATIONS

3.1 Estimates from the density and velocity profiles

To date, there are two standard methods to estimate concentrations in dark matter halos extracted from N-body simulations.

The first method tries to directly estimate the density profile. It takes all the particles in the halo and bins them in the logarithm of the radial coordinate from the halo center. Then, it estimates the density in each logarithmic bin counting the particles and dividing by the corresponding shell volume. At this point is is possible to make a direct fit to the density as a function of the radial coordinate. This method has been **used broadly for more than two decades** to study the mass-concentration-redshift relation of dark matter halos using the Millennium Simulation Series.

no veo la necesidad de citar el "trabajo mas" reciente que usa el metodo, cuando ha sido usado durante mas de dos decadas!

A second method uses the circular velocity profile. It finds the value of x for which the normalized circular velocity $v(<x)$ shows a maximum. Using this value it solves numerically for the corresponding value of the concentration using Eq. (7). This method has been most recently used by Klypin et al. (2014) to study the mass-concentration-redshift relation using the Multidark Simulation Suite.

3.2 Our proposal: estimate from the integrated mass profile

Our method uses the integrated mass profile. First we define the center of the halo to be at the position of the particle with the lowest gravitational potential. Then we rank the particles by their increasing radial distance from the center. From this ranked list of $i = 1, N$ particles, the total mass at a radius r_i is $M_i = i \times m_p$, where r_i is the position of the

i-th particle and m_p is the mass of a single computational particle. In this process we discard the particle at the center.

We divide the enclosed mass mass M_i and the radii r_i by their virial values to obtain the dimensionless variables m_i and x_i. Once the mass profile is expressed in dimensionless variables the concentration is the only free parameter. We use an Affine Invariant Markov chain Monte Carlo implemented in the python module *emcee* (Foreman-Mackey et al. 2013) to sample the likelihood function distribution defined by $\mathcal{L}(c) \propto \exp(-\chi^2(c)/2)$ where the $\chi^2(c)$ is written as

$$\chi^2(c) = \sum_{i=1}^{N} [\log m_i - \log m(<x_i; c)]^2, \qquad (8)$$

where $m(<x_i; c)$ corresponds to the values in Eq.(3) at $x = x_i$ for a given value of the concentration parameter c and the i index sums over all the particles in the numerical profile. From the χ^2 distribution we find the optimal value of the concentration and its associated uncertainty.

The construction of the numerical integrated mass profile has two advantages with respect to the density and velocity methods, it does not involve any binning (unlike the density methods) and the sampling method uses the information from all the particles in the halo (unlike the velocity method).

4 RESULTS

We now present the results of applying the three methods above mentione on two different halo samples. The first sample is composed by mock halos generated to have known concentration values in perfect spherical symmetry following an NFW profile. We use this sample to check that we can recover the expected values but also gauge the impact of the number of particles on the outcomes. The second sample comes from a publicly available N-body cosmological simulation. From this sample we quantify again the differences between all the methods and also estimate the impact on the mass-concentration relationship.

4.1 Mock halo sample

The method we use to generate the mock halos is based on the integrated mass profile. We start by fixing the desired concentration c and total number of particles N in the mock halo. With these values we define the mass element as $\delta m = 1/M$, corresponding to the mass of each particle such that the total mass is one. Then for each particle, $i = 1, \ldots, N$, we find the value of r_i such that the difference

$$m(<r_i; c) - i \cdot \delta m \qquad (9)$$

is zero using Ridders' method.

The value of r_i is the radius of the i-th particle of the mock halo. Then we generate random polar and azimuthal angles θ and ϕ for each particle to ensure spherical symmetry. Finally these three spherical coordinates are transformed into Cartesian coordinates $(r, \theta, \phi) \rightarrow (x, y, z)$.

We generate in total 400 mock halos split into four different groups of 100 halos each. The four groups differ in

the total number of particles for their halos: 20, 200, 2000 and 20000. Inside each group the halos have random concentration values in the range $1 < c < 20$ with a uniform distribution. For all these halos **ww?** the concentration values using the density, velocity and mass methods described in the previous section. We quantify the difference between the expected c_{in} and obtained c_{out} values by

$$D = (c_{in} - c_{out})/c_{in}, \tag{10}$$

and

$$\langle |D| \rangle = \frac{1}{|\mathcal{H}|} \sum_{\mathcal{H}} |D|, \tag{11}$$

where $\mathcal{H}$ corresponds to a set of mock halos, and $|\mathcal{H}|$ is the number of haloes in $\mathcal{H}$. **The larger the value of $\langle |D| \rangle$, the larger the discrepace of the concentrations obtained for that method**

Figure 1 shows the behaviour of $\langle |D| \rangle$ as a function of halo particle number for the three different methods to estimate the concentration.

At fixed particle numbers our method always shows the lowest $\langle |D| \rangle$ values compared to the other two methods. Its accuracy is on the order of 10% for 20 particles in the halo, going down to 0.01% for halos with 20000 particles. The dependence of $\langle |D| \rangle$ with the particle number N goes approximately as $\langle |D| \rangle \propto N^{-1/2}$, hinting that the accuracy of the method is related to a decrease of Poisson noise.

The method based on the maximum of the circular velocity shows a similar behaviour $\langle |D| \rangle \propto N^{-1/2}$. Its accuracy is $2-5$ times less than in our method, on the order of 20% for 20 particle halos and 0.5% for 20000 particle halos. **The method based on the direct density fit shows the lowest accuracy for a low particle number. As it is discussed in (Muñoz-Cuartas et al. 2011), density binning for halos with particle numbers below ~ 200 leads to a biased estimation of the mass density profile, and therefore to a biased estimation of the concentration parameter. This behaviour is evident in the large values of $\langle |D| \rangle$ for halos with number of particles below 200 and an intermediate accuracy between the other two methods for a high particle number.**

4.2   Halos from a cosmological simulation

The results presented in the previous section show that in an idealized setup (perfect spherical halos, pure NFW desity profiles, total isolation) our method of the mass profile performs better than the other two methods commonly used to measure concentrations in simulated dark matter haos. However, actual simulated dark matter halos are much more complex. They are not isolated, many of them experience mergers that take them out of the equilibrium. Halos may have also plenty of substructure, etc. All these effects disturb the mass density profile, taking it away from the ideal NFW profile we assume in this wok. In order to see the real performance of our new method use it to estimate the concentration parameter in dark matter halos obtained from a cosmological Nbody simulation and compare with the other two calsical methods.

We use data from the MultiDark cosmological simulation that follows the non-linear evolution of a dark matter density field sampled with 2048^3 particles over a cubic box of 1000 h^{-1}Mpcon a side. The data is publicly available through http://www.cosmosim.org/. More details about the structure of the database and the simulation can be found in (Riebe et al. 2013).

We build a sample of all halos located in a cubic subvolume of 100 h^{-1}Mpcon a side centered on the most massive halo in the simulation at $z = 0$ which corresponds to the miniMDR1 tables in the database. From this sample we select all the halos at $z = 0$ detected with a Friends-of-Friends (FoF) algorithm with masses in the interval $10^{12} \leqslant M_{\rm FoF}/h^{-1}{\rm M}_\odot \leqslant 10^{15}$. The FoF algorithm used with a linking length of 0.17 times the **mean** inter-particle distance. This choice translates into an overdensity $\Delta_h \sim 400 - 700$ dependent on the halo concentration (More et al. 2011). Finally, we select from the database all the particles that belong to each FoF group.

From this set of particles we follow the procedure spelled out in Section 3 with $\Delta_h = 740$ (corresponding to 200 times the critical density) to select an spherical region that we redefine to be our halo. This choice makes that our overdensities are fully included inside the original FoF particle group. On the interest of providing a fair comparison against the density method we only report results from overdensities with at least 200 particles.

Figure 3 shows the results of the mass-concentration relationship.

Aqui hay algo importante que hay que entender antes de discutir esta grfica , y es la razn por la cual el metodo del perfil de masa da valores de concentracin tan bajos a baja masa y comparables a los de los otros dos mtodos a alta masa. Es importante entender la razn de esto!. Se me ocurren unas preguntas para tratar de entender.
1) La grafica de c-M 3 usa todos los halos o solo los halos relajados? La inclusin de halos no relajados introduce in bias en la mediana en Cvir, as que vale la pena inclusive agregar una linea mas a la grfica con los halos relajados y sin ellos. Para los otros dos mtodos ya se sabe que hace la poblacin de halos no relajados en la medida as que no creo necesario agregarlas para esos mtodos.
Hay que explicar un poco mas la grfica en el sentido de que se grafica y como se calcul. mean concentration?, Median concentrations? o mean in logscale? Mas bins de cuanto? Mnimo cuantos halos por mass bin?, Halos relajados en todos los casos, o indistintos?

5   CONCLUSIONS

In this paper, we presented a new method to estimate the concentration of dark matter halos in N-body simulations. We tested our method on mock halo data to study the impact of total number of particles and input concentration on the retrieved values. We compared these results against two other methods commonly used in the literature to estimate concentrations. Finally, we applied our method to halos extracted from a cosmological N-body simulation to estimate the impact of our method on the mass concentration relationship.

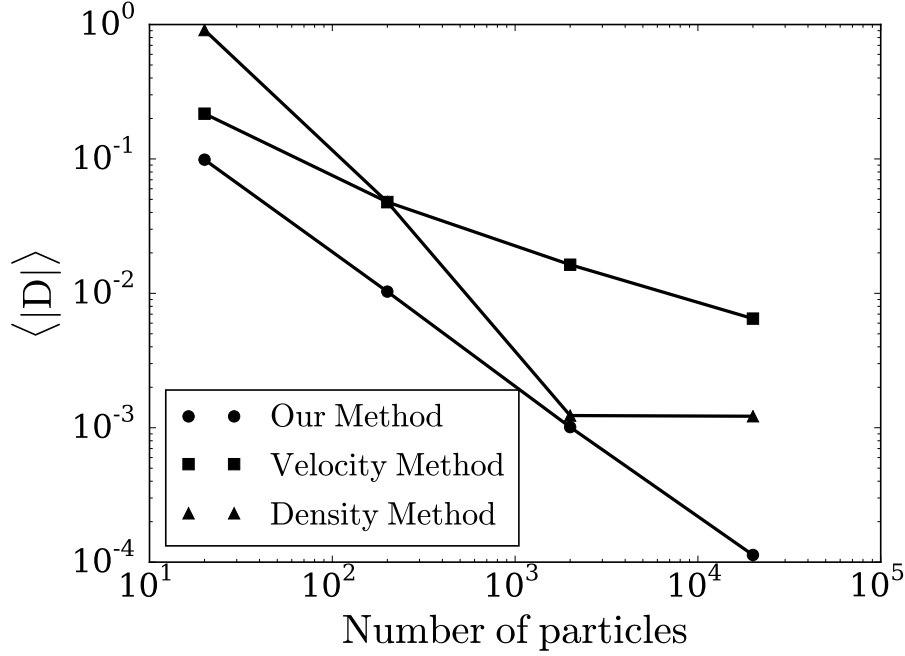The first benchmark was performed on mock halos gen-

Figure 1. Average value of the relative error in the concentration estimate, $\langle|D|\rangle$, as a function of the particle number N in the set of mock halos. Different symbols represent different methods. Our method provide the most accurate estimate at fixed particle number N. *Con respecto a esta figura tengo una pregunta. Yo ajust los perfiles con menos de 200 partulas? no recuerdo!*
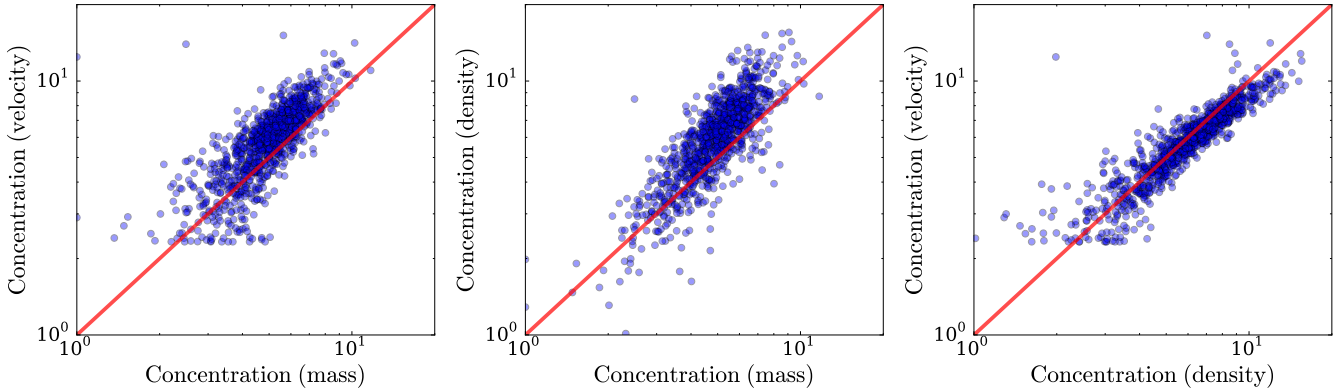

Figure 2. Comparison between the concentrations measured by our method and the maximum velocity (left) and density (middle) methods. The line indicates the equal value between the two techniques. The right panel compares the results of the maximum velocity and density methods.

erated with known concentration values for different particle numbers. For all methods, the accuracy in retrieving the input concentration increases with the number of particles as summarized in Figure 1. Our method systematically shows smaller errors in the retrieved values compared to the other two methods, going from 10% for halos with 20 particles down to 0.01% for halos with 2×10^4 particles. In our method the average error on the retrieved values decreases with the number of particles as $\langle|D|\rangle \propto N^{-1}$. The error in density method initially behaves as $\langle|D|\rangle \propto N^{-3/2}$ but at $N = 2 \times 10^3$ it saturates to 0.1%. For the velocity method the error behaves closely to $\langle|D|\rangle \propto N^{-1/2}$. We also gauged the effect of different concentration parameters at fixed particle numbers. We found larger offsets for larger input concentrations. The offset goes in the sense that the measured concentration tends to be underestimated. Nevertheless, the dominant effect on the measurement is the particle number.

We used a N-body cosmological simulation to test the impact of our method on the mass-concentration relationship. Although the three methods are in general agreement there are noticeable differences in the mass concentration relationship.
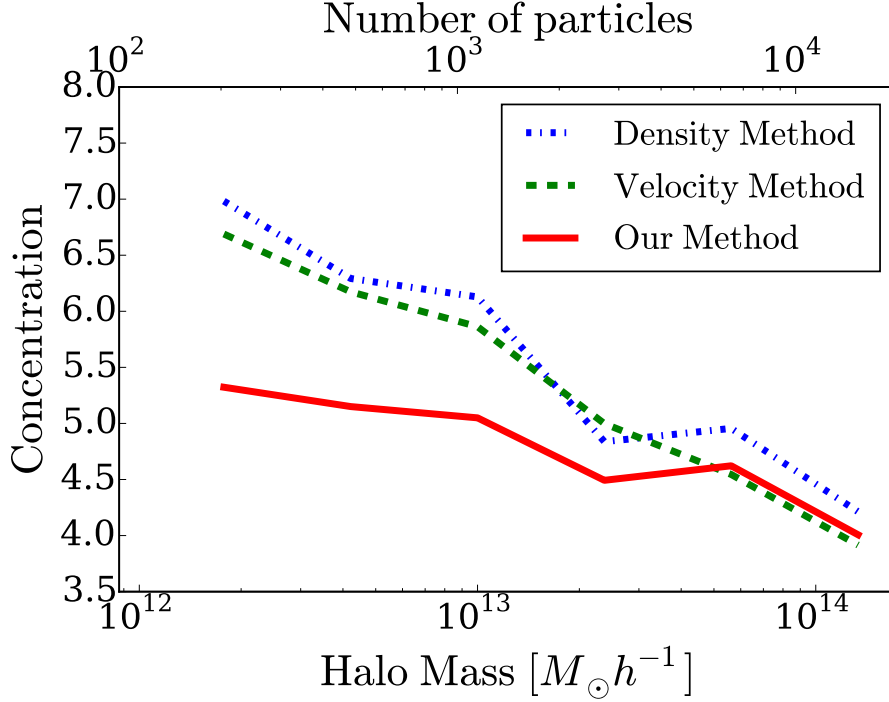
Figure 3. Mass-concentration relationship for the three different methods used on the same cosmological N-body data. The lines correspond to the median concentration values in each bin.

REFERENCES

Buote D. A., Gastaldello F., Humphrey P. J., Zappacosta L., Bullock J. S., Brighenti F., Mathews W. G., 2007, ApJ, 664, 123

Comerford J. M., Natarajan P., 2007, MNRAS, 379, 190

Duffy A. R., Schaye J., Kay S. T., Dalla Vecchia C., 2008, MNRAS, 390, L64

Foëx G., Motta V., Jullo E., Limousin M., Verdugo T., 2014, A&A, 572, A19

Foreman-Mackey D., Hogg D. W., Lang D., Goodman J., 2013, PASP, 125, 306

Giocoli C., Meneghetti M., Metcalf R. B., Ettori S., Moscardini L., 2014, MNRAS, 440, 1899

Klypin A., Yepes G., Gottlober S., Prada F., Hess S., 2014, ArXiv e-prints

Klypin A. A., Trujillo-Gomez S., Primack J., 2011, ApJ, 740, 102

Ludlow A. D., Navarro J. F., Angulo R. E., Boylan-Kolchin M., Springel V., Frenk C., White S. D. M., 2014, MNRAS, 441, 378

Mandelbaum R., Seljak U., Hirata C. M., 2008, JCAP, 8, 6

More S., Kravtsov A. V., Dalal N., Gottlöber S., 2011, ApJS, 195, 4

Muñoz-Cuartas J. C., Macciò A. V., Gottlöber S., Dutton A. A., 2011, MNRAS, 411, 584

Navarro J. F., Frenk C. S., White S. D. M., 1997, ApJ, 490, 493

Neto A. F., Gao L., Bett P., Cole S., Navarro J. F., Frenk C. S., White S. D. M., Springel V., Jenkins A., 2007, MN-RAS, 381, 1450

Prada F., Klypin A. A., Cuesta A. J., Betancort-Rijo J. E., Primack J., 2012, MNRAS, 423, 3018

Riebe K., Partl A. M., Enke H., Forero-Romero J., Gottlöber S., Klypin A., Lemson G., Prada F., Primack J. R., Steinmetz M., Turchaninov V., 2013, Astronomische Nachrichten, 334, 691

Shan H., Kneib J.-P., Li R., Comparat J., Erben T., Makler M., Moraes B., Van Waerbeke L., Taylor J. E., Charbonnier A., 2015, ArXiv e-prints

Springel V., White S. D. M., Jenkins A., Frenk C. S., Yoshida N., Gao L., Navarro J., Thacker R., Croton D., Helly J., Peacock J. A., Cole S., Thomas P., Couchman H., Evrard A., Colberg J., Pearce F., 2005, Nature, 435, 629

Taylor J. E., Navarro J. F., 2001, ApJ, 563, 483